1-4-2008

Differential Role of $NADP^+$ and NADPH in the Activity and Structure of GDP-D-mannose 4,6-Dehydratase from Two Chlorella Viruses

Floriana Fruscione
University of Genova

Laura Sturla
University of Genova

Garry Duncan
Nebraska Wesleyan University, gduncan@nebrwesleyan.edu

James L. Van Etten
University of Nebraska-Lincoln, jvanetten1@unl.edu

Paola Valbuzzi
University of Nebraska - Lincoln

See next page for additional authors

THE JOURNAL OF BIOLOGICAL CHEMISTRY VOL. 283, NO. 1, pp. 184–193, January 4, 2008

Differential Role of $NADP^+$ and NADPH in the Activity and Structure of GDP-D-mannose 4,6-Dehydratase from Two Chlorella Viruses*[S]

Received for publication, August 9, 2007, and in revised form, October 9, 2007 Published, JBC Papers in Press, November 1, 2007, DOI 10.1074/jbc.M706614200

Floriana Fruscione[‡], Laura Sturla[‡], Garry Duncan[§], James L. Van Etten[¶], Paola Valbuzzi[¶], Antonio De Flora[‡], Eleonora Di Zanni[‡], and Michela Tonetti[‡1]

From the [‡]Department of Experimental Medicine, University of Genova and Center of Excellence for Biomedical Research, Viale Benedetto XV, 1, 16132, Genova, Italy, [§]Department of Biology, Nebraska Wesleyan University, Lincoln, Nebraska 68504-2794, and [¶]Department of Plant Pathology and Nebraska Center for Virology, University of Nebraska, Lincoln, Nebraska 68583-0722

GDP-D-mannose 4,6-dehydratase (GMD) is a key enzyme involved in the synthesis of 6-deoxyhexoses in prokaryotes and eukaryotes. *Paramecium bursaria* chlorella virus-1 (PBCV-1) encodes a functional GMD, which is unique among characterized GMDs because it also has a strong stereospecific NADPH-dependent reductase activity leading to GDP-D-rhamnose formation (Tonetti, M., Zanardi, D., Gurnon, J., Fruscione, F., Armirotti, A., Damonte, G., Sturla, L., De Flora, A., and Van Etten, J.L. (2003) *J. Biol. Chem.* 278, 21559–21565). In the present study we characterized a recombinant GMD encoded by another chlorella virus, *Acanthocystis turfacea* chlorella virus 1 (ATCV-1), demonstrating that it has the expected dehydratase activity. However, it also displayed significant differences when compared with PBCV-1 GMD. In particular, ATCV-1 GMD lacks the reductase activity present in the PBCV-1 enzyme. Using recombinant PBCV-1 and ATCV-1 GMDs, we determined that the enzymatically active proteins contain tightly bound NADPH and that NADPH is essential for maintaining the oligomerization status as well as for the stabilization and function of both enzymes. Phylogenetic analysis indicates that PBCV-1 GMD is the most evolutionary diverged of the GMDs. We conclude that this high degree of divergence was the result of the selection pressures that led to the acquisition of new reductase activity to synthesize GDP-D-rhamnose while maintaining the dehydratase activity in order to continue to synthesize GDP-L-fucose.

GDP-D-mannose 4,6-dehydratase (GMD,[2] EC 4.2.1.47) is the first enzyme in the biosynthetic pathways that leads to the formation of several deoxyhexoses, such as GDP-L-fucose (1), GDP-D-rhamnose (2), GDP-6-deoxy-D-talose (3), and GDP-D-perosamine (4). Genes encoding GMDs have been identified in most prokaryotes and eukaryotes (5–8). Recently, we characterized the first GMD encoded by a virus, *Paramecium bursaria* chlorella virus 1 (PBCV-1) (9). PBCV-1 is the prototype of a group (family Phycodnaviridae) of large, icosahedral, plaque-forming, double-stranded DNA viruses that replicate in certain unicellular, eukaryotic chlorella-like green algae (10). In nature, the chlorella host is a hereditary endosymbiont in the ciliated protozoan *P. bursaria*. PBCV-1 has ~365 protein-encoding genes, including genes that encode several proteins that resemble enzymes involved in the metabolism and processing of sugars; these proteins include five putative glycosyltransferases believed to be involved in the glycosylation of the virus major capsid protein (11). PBCV-1 also encodes the two enzymes involved in GDP-L-fucose biosynthesis, GMD and GDP-4-keto-6-deoxy-D-mannose epimerase/reductase (GMER) (Fig. 1) (9).

GMD is a member of the short-chain dehydrogenase/reductase family of proteins (12) and in general has structural features compatible with enzymes belonging to the reductase-epimerase-dehydrogenase superfamily (13). GMD sequences are well conserved among organisms; they all contain three conserved amino acids, Ser/Thr, Tyr, and Lys, involved in catalysis and a glycine-rich motif at the N terminus that is involved in cofactor binding. GMD three-dimensional structures have been reported from several organisms (14–17). GMD binds its coenzyme NADP(H) in the N-terminal domain, which consists of a seven-stranded Rossman fold, whereas the C-terminal domain is involved in substrate binding. The PBCV-1 GMD crystal structure was determined at 3.8 Å resolution (17), and its tertiary structure resembles other GMDs. However, the low resolution of the PBCV-1 crystals did not provide definitive information on the structure of the active site nor did it allow the identification of the redox state of the coenzyme.

The catalytic mechanism proposed for GMD is similar to that reported for other nucleotide sugars dehydratases, such as dTDP-D-glucose dehydratase and CDP-D-glucose dehydratase (18–19). The presence of an oxidized coenzyme ($NADP^+$ in the case of GMD) is required for the beginning of the catalytic cycle. Initially, a hydride is transferred from C-4 of the mannose moiety to $NADP^+$, which is accordingly reduced to NADPH, with the formation of a 4-keto-intermediate (14). At this stage

* This work was supported in part by FIRB Project RBNE01T8C8 "Riconoscimento Molecolare e Funzionalità Cellulare" and PRIN Project 2003 (to M. T.), Public Health Service Grant GM32441 (to J. L. V.-E.) and National Institutes of Health Grants P21RR15635 and P20RR016469 from the COBRE program (to J. V. E.), and the INBRE program (to G. D.) of the National Center for Research Resources. The costs of publication of this article were defrayed in part by the payment of page charges. This article must therefore be hereby marked "*advertisement*" in accordance with 18 U.S.C. Section 1734 solely to indicate this fact.

[S] The on-line version of this article (available at http://www.jbc.org) contains supplemental Figs. 1–4.

[1] To whom correspondence should be addressed. E-mail: tonetti@unige.it.

[2] The abbreviations used are: GMD, GDP-D-mannose 4,6-dehydratase; PBCV-1, *P. bursaria* chlorella virus 1; ATCV-1, *A. turfacea* chlorella virus 1; GMER, GDP-4-keto-6-deoxy-D-mannose epimerase/reductase; DTT, dithiothreitol; SEC, size exclusion chromatography; PBS, phosphate-buffered saline; HPLC, high performance liquid chromatography.

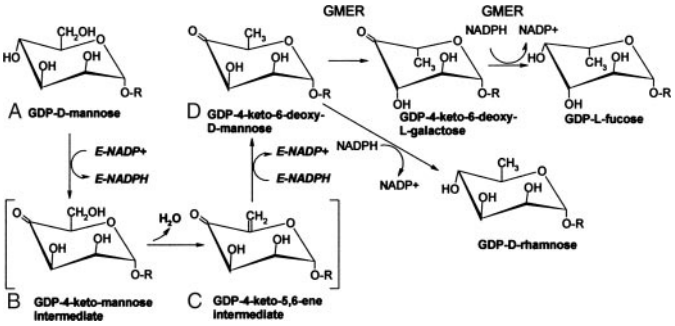

FIGURE 1. **Biosynthetic pathway of GDP-L-fucose from GDP-D-mannose.** GDP-D-mannose is converted to GDP-4-keto-6-deoxy-D-mannose by GMD. One proposed mechanism of dehydration is shown in *brackets*. A hydride is transferred from C-4 of GDP-D-mannose (*A*) to protein bound $NADP^+$ ($E\text{-}NADP^+$), which becomes reduced, to form a 4-keto-intermediate (*B*). A water molecule is lost with the formation of 4-keto-5,6-ene intermediate (*C*). Protein-bound NADPH (*E-NADPH*) reduces C-6 with consequent formation of GMD final product (*D*) and regeneration of $E\text{-}NADP^+$. GDP-4-keto-6-deoxy-D-mannose then undergoes an epimerization and a NADPH-dependent reduction, both catalyzed by GMER, to form GDP-L-fucose. Alternatively, GDP-4-keto-6-deoxy-D-mannose can undergo a NADPH-dependent reduction catalyzed by PBCV-1 GMD to form GDP-D-rhamnose.

two different mechanisms have been proposed; a proton is removed from C-5 by a base on the enzyme followed by dehydration of the 4-keto-intermediate between C-5 and C-6 yielding a 4-keto-5,6-ene species. In the second mechanism a 4-ene-diol/enolate species is formed in the second step of the reaction. In both cases a conserved acid residue (Glu-135 in *Escherichia coli* sequence) has been proposed to act as a base that removes a proton from C-6 (14). The final step in the reaction involves a hydride transfer from bound NADPH to C-6 of the sugar, leading to the product GDP-4-keto-6-deoxy-D-mannose and regeneration of $NADP^+$. GDP-4-keto-6-deoxy-D-mannose is the substrate for GMER; however, it is not a very stable compound. Thus, the presence of an oxidized coenzyme is an absolute requirement for initiating GMD activity. However, structural data obtained by x-ray crystallography indicated that both *Arabidopsis thaliana* and *Pseudomonas aeruginosa* GMD contain only tightly bound NADPH instead of $NADP^+$ (15–16). Preliminary data obtained in our laboratory also indicate that NADPH is present in recombinant GMD from virus PBCV-1.[3]

The PBCV-1 recombinant GMD differs from other currently characterized GMDs because, in addition to the dehydratase activity, the protein also has a strong stereospecific NADPH-dependent reductase activity that produces GDP-D-rhamnose (9). The low resolution of the active site in the PBCV-1 GMD crystals (17) did not provide any information that would explain the high reductase activity of the enzyme. However, a reductase activity implies an exchange between the oxidized form of the bound coenzyme and the exogenous NADPH added to the reaction mixture.

Recently, the genome of another virus (*Acanthocystis turfacea* chlorella virus (ATCV-1)) that infects *Chlorella* SAG 3.83 was sequenced (20). ATCV-1 also contains genes encoding putative GMD and GMER enzymes. However, the GMD amino acid sequences from ATCV-1 and PBCV-1 only have 53% identity, suggesting the two enzymes have undergone significant divergence and that they might have different properties.

To address the presence and possible role of NADPH in the structural and catalytic properties of GMD, we expressed GMD from both PBCV-1 and ATCV-1 viruses and analyzed their kinetic and structural properties, their coenzyme content, and their coenzyme binding affinities. The results described here indicate that the ATCV-1 protein has dehydratase activity on GDP-D-mannose, but that it lacks the reductase activity present in PBCV-1 GMD. Moreover, we demonstrate that the catalytically active forms of both proteins contain NADPH, which is essential for stabilizing the enzyme structure. We propose that the presence of NADPH in these two dehydratases, even if not involved in the catalytic process, is not incidental but that it serves an important role in enzyme function.

EXPERIMENTAL PROCEDURES

Expression and Purification of Recombinant GMD Proteins—GMD proteins were expressed in *E. coli* as glutathione *S*-transferase fusion proteins as previously described (9) using pGEX-6P1 vector (GE Healthcare). The ATCV-1 GMD sequence corresponds to open reading frame Z804L in ATCV-1 genome (GenBank™ accession number EF101928). Purification to homogeneity was achieved by chromatography on a GSH-Sepharose 4B column followed by *in situ* proteolytic cleavage of the tag by Prescission Protease (GE Healthcare). The proteins were concentrated to about 4–6 mg/ml using a Centricon YM-10 system (Amicon-Millipore) and stored at 4 °C in 50 mM Tris-HCl, 150 mM NaCl, 1 mM EDTA, pH 7.0 (TBSE) containing 1 mM dithiothreitol (DTT). ApoGMDs were prepared after preincubation of the proteins with GDP-4-keto-6-deoxy-D-mannose followed by dialysis against 1000 volumes of TBSE/DTT. This treatment resulted in complete removal of bound coenzymes (see below).

Protein concentrations were determined by UV_{280} absorbance of the purified proteins in 6 M guanidine hydrochloride, 0.02 M phosphate buffer, pH 6.5, using a calculated extinction coefficient of 47,330 M^{-1} cm^{-1} for PBCV-1 GMD and 51,340 M^{-1} cm^{-1} for ATCV-1 GMD (21). Because the holoenzyme contains bound NADP(H), which can interfere with the UV_{280} assay, protein concentrations were also determined by the Bradford procedure (Bio-Rad) using apoGMD as a standard. GMD concentration was expressed as molarity of the monomer form of the protein. Protein purity, monitored by SDS-PAGE, exceeded 95% in all preparations.

Determination of GMD-bound $NADP^+$/NADPH—The amounts of protein-bound $NADP^+$ and NADPH were determined by reverse phase HPLC on either untreated purified GMD or after preincubation of the proteins (100 μM) with a molar excess of GDP-4-keto-6-deoxy-D-mannose (150 μM). This latter treatment converts all bound NADPH to the oxidized form (see below). Aliquots of both the untreated and treated proteins were dialyzed to verify coenzyme release from GMD. The concentrated protein (100 μM) was then dialyzed against 1000 volumes of TBSE/DTT for 24 h at 4 °C.

To discriminate between $NADP^+$ and NADPH, the proteins were subjected to treatments that selectively destroy the oxidized and reduced forms of NADP before analysis (22). For

[3] M. Tonetti, E. Di Zanni, L. Sturla, and F. Fruscione, unpublished results.

$NADP^+$ determination, 100 μl of protein solution (50 μM, expressed as the monomer) or $NADP^+$/NADPH standards in TBSE buffer were first treated with 10 μl of 3.7 M $HClO_4$. Samples were then neutralized with 3 M K_2CO_3, and the precipitate was removed by centrifugation; 100 μl of supernatant were diluted 1:1 with TBSE and subjected to HPLC analysis. For NADPH determination, 5 μl of 4 N NaOH were added to 100 μl of proteins or standards in TBSE; samples were heated at 70 °C for 10 min and immediately chilled in ice. These solutions were then neutralized by adding 4 N HCl and centrifuged. The supernatants were diluted as described above.

HPLC analysis was performed with an HP 1090 apparatus (Agilent) equipped with a Diode Array Detector and fitted with a reverse phase C18 column (25 × 300 cm, 5-μm particle size, Waters) as described (23). The eluate was monitored at 260 and 340 nm. Concentrations of NADP(H) (obtained from Sigma) were determined using an extinction coefficient of 17,800 M^{-1} cm^{-1} at 260 nm for $NADP^+$ and an extinction coefficient of 6,220 M^{-1} cm^{-1} at 340 nm for NADPH. HPLC analysis of standard NADPH revealed no contamination by the oxidized form. Coenzyme concentrations in the samples were obtained by linear regression using the Prism 5.0 program (Graphpad).

Fluorescence Analyses—All fluorescence measurements were performed at 22 °C using a PerkinElmer Life Sciences LS50B spectrofluorimeter in a 0.5 × 0.5-cm quartz cuvette. Emission spectra were recorded with freshly diluted protein to a 1 μM concentration in PBS, pH 7.3, from a 100 μM either untreated or GDP-4-keto-6-deoxy-D-mannose-treated GMD solution. After dilution, protein solutions were allowed to equilibrate until reaching stable fluorescence intensities. Enzyme-bound NADPH was determined using the excitation wavelength at 350 nm (5-nm slit width) and recording fluorescence emission from 370 to 600 nm (10-nm slit width). Intrinsic tryptophan fluorescence and fluorescence energy transfer were measured with an excitation of 295 nm (5-nm slit width) while monitoring emission from 310 to 500 nm (10-nm slit width). Sample spectra were corrected for background and Raman scattering by subtracting buffer spectra.

Fluorescence titration experiments were used to determine the binding affinities of the cofactors to the apoenzymes. Protein concentrations in PBS were 500 nM for both $NADP^+$ and NADPH titrations. Solutions were prepared immediately before use, and the concentrations were determined as described above. $NADP^+$ binding to protein was monitored by quenching of tryptophan fluorescence at 340 nm after excitation at 295 nm; quenching indicates cofactor binding to the apoenzyme. NADPH binding to the apoprotein was monitored by enhancement of fluorescence emission at 440 nm (excitation 350 nm). Each fluorescence value measured in the presence of the protein was corrected by subtracting the contribution of unbound NADPH to the fluorescence. Inner filtering effects were determined to be negligible at the enzyme and NADPH concentrations used. For experiments involving higher concentrations of $NADP^+$ the following correction was applied as described (24),

$$F_c = F_{obs} \times 10^{((A_{ex} + A_{em})/2)} \quad \text{(Eq. 1)}$$

where F_c is the corrected intensity, F_{obs} is the observed intensity, and A_{ex} and A_{em} are the absorbance of sample at the excitation and emission wavelengths, respectively.

Dissociation constants (K_D) were determined by plotting the corrected change in emission (ΔF) against the concentration of the titrant. The Prism 5.0 program (GraphPad) was used to fit the data by nonlinear regression. For $NADP^+$ titration, data best fit a single binding site equation (Equation 2), where ΔF is the change in fluorescence, ΔF_{max} is the maximal change in fluorescence, and X is the concentration of the titrant,

$$\Delta F = (\Delta F_{max} \times X)/(K_D + X) \quad \text{(Eq. 2)}$$

Conversely, data obtained after NADPH titration of both PBCV-1 and ATCV-1 apoenzymes best fit one-site binding by the Hill equation (Equation 3), where ΔF is the change in fluorescence, ΔF_{max} is the maximal change in fluorescence, × is the concentration of the titrant, and h is the Hill slope,

$$\Delta F = (\Delta F_{max} \times X^h)/(K_D + X^h) \quad \text{(Eq. 3)}$$

Size-exclusion Chromatography—The molecular mass of GMD proteins was determined by size exclusion chromatography (SEC) using a TSKgel G3000SWXL column, 7.8 × 300 mm, 5-μm particle size (Tosoh Biosciences). The mobile phase was 0.1 M sodium phosphate buffer, pH 6.7, containing 0.1 M Na_2SO_4. The eluate was monitored at 220 nm. The following proteins were used as standards: cytochrome C (12 kDa), carbonic anhydrase (29 kDa), ovalbumin (44 kDa), bovine serum albumin (66 kDa), γ-globulin (157 kDa), and tyroglobulin (670 kDa). All protein standards were obtained from Sigma. Blue dextran and DTT were used to determine the void and total column volumes, respectively, to enable calculation of the distribution coefficient K_{av} according to the following equation (25),

$$K_{av} = (V_e - V_o)/(V_t - V_o) \quad \text{(Eq. 4)}$$

where V_e is the elution volume of the protein, V_o the column void volume, and V_t is the total bed volume. The K_{av} for each protein standard was plotted against the logarithm of the corresponding molecular mass. K_{av} of samples was used to calculate the molecular mass by linear regression analysis.

Analysis of Enzyme Activities—GMD dehydratase activity was assayed in TBSE containing 1 mM DTT. A mixture of GDP-D-[U-^{14}C]mannose (GE Healthcare; specific activity 11.1 GBq/mmol) and unlabeled GDP-D-mannose (Sigma) was used as substrate at a final specific activity of 1.4 GBq/mmol. Assays were conducted at 37 °C, and aliquots were withdrawn at various times. Reactions were stopped by adding 10-μl samples to 90 μl of ice-cold water followed by extraction with sodium perchlorate/potassium acetate as previously described (26). The conversion of GDP-D-[^{14}C]mannose to GDP-4-keto-6-deoxy-D-[^{14}C]mannose was used to measure ATCV-1 GMD dehydratase activity; the two sugar nucleotides were detected by reverse phase HPLC followed by continuous flow scintillation counting as described previously (9). For the experiments with PBCV-1 proteins in the presence of NADPH, where both GDP-4-keto-6-deoxy-D-mannose and GDP-D-rhamnose are formed, activity was determined by following GDP-D-mannose consumption. GMD reductase activity was carried out in the same

conditions using different concentrations of NADPH and GDP-4-keto-6-deoxy-D-[^{14}C]mannose as substrate. GDP-4-keto-6-deoxy-D-[^{14}C]mannose was produced from GDP-D-mannose using the GMD dehydratase activity in the absence of added NADPH. Complete conversion of GDP-D-mannose to GDP-4-keto-6-deoxy-D-mannose was followed by HPLC. The sugar nucleotide was separated from GMD by ultrafiltration using the Microcon YM-10 system (Amicon-Millipore). Heat-inactivation of GMD was avoided, as we observed a significant degradation of the product.

Phylogenetic Analyses—BLASTP searches for PBCV-1 GMD (AAO67555) and PBCV-1 GMER (AAC96663) were conducted to construct two phylogenetic trees. Twenty taxa, including prokaryotes, eukaryotes, Archaea, as well as one virus were selected. The 20 taxa, which included PBCV-1 and ATCV-1, were aligned with ClustalW using the default setting in the Biology Workbench. The alignments were converted to NEXUS format and imported into PAUP 4.0b10 (27) for phylogenetic analysis. Trees were constructed using the following three methods: maximum parsimony heuristic, neighbor joining, and maximum parsimony bootstrap (1000 replicates). Because the PBCV-1 GMD and GMER proteins have sequence homology to one another, they were used as the out-groups to root the two trees; *i.e.* PBCV-1 GMER was used to root the GMD tree, whereas PBCV-1 GMD was used to root the GMER tree. The GMD tree shown in Fig. 7 is a summary of the very similar tree topologies from the three tree-building methods. The values on the branches are the percentage of bootstrap support (1000 replicates). Only bootstrap values >50% are reported.

RESULTS

Determination of Bound NADP$^+$/NADPH—The catalytic mechanism proposed for GMDs requires NADP$^+$ as the coenzyme to initiate the reaction. However, several observations indicate that NADPH is also tightly bound to the enzyme (15–16). Likewise, incubating GDP-4-keto-6-deoxy-D-mannose with equimolar amounts of purified recombinant PBCV-1 and ATCV-1 GMDs results in the appearance of GDP-D-rhamnose without adding exogenous NADPH (results not shown). These results suggest that NADPH is present and catalytically competent in the two recombinant viral GMDs. To address the presence and the possible role of NADPH in GMD activity, we measured the coenzyme content in the two proteins by HPLC (supplemental Figs. 1 and 2). To discriminate between NADPH and NADP$^+$, the recombinant proteins were isolated under conditions that selectively destroy either the oxidized or the reduced form of the coenzyme. The HPLC analysis also revealed another substance(s) bound to the purified proteins that has a spectrum suggestive of a guanylate moiety (supplemental Figs. 1, *A* and *B*, and 2, *A* and *B*). For ATCV-1 GMD, variable amounts of NADP$^+$ and NADPH were detected with different enzyme preparations (Table 1); these results indicate that the ATCV-1 protein contains both forms of the coenzyme. However, in all cases the additive amount of NADP$^+$ and NADPH was about 1 mol/mol of monomeric ATCV-1 protein. In contrast, PBCV-1 GMD contained primarily NADPH, and only trace amounts of NADP$^+$ were detected (Table 1).

TABLE 1

Determination of GMD-bound NADP$^+$ and NADPH

NADP$^+$ and NADPH concentrations were determined by HPLC, as described under "Experimental Procedures" using either freshly purified protein or after preincubation of the enzymes with GDP-4-keto-6-deoxy-D-mannose.

	PBCV-1 GMD		ATCV-1 GMD	
	NADP$^+$	NADPH	NADP$^+$	NADPH
	μmol/mol of protein monomer			
Native GMD	0.03 ± 0.01	0.87 ± 0.15	0.25–0.45[a]	0.57–0.73[a]
Native GMD + GDP-4-keto-6-deoxy-D-mannose	0.85 ± 0.10	0.07 ± 0.02	0.92 ± 0.12	0.06 ± 0.03

[a] For ATCV-1 GMD, the ratio between NADP$^+$ and NADPH varied considerably between enzyme preparations, but in all cases the total amount of the coenzymes was close to 1 mol/each mol of monomer. As a consequence, the range of coenzyme concentrations was reported instead of the mean. All other data are the means of coenzyme content derived from at least three recombinant protein preparations.

Incubating the two viral GMDs with GDP-4-keto-6-deoxy-D-mannose led to almost total conversion of NADPH to NADP$^+$, resulting in about 1 mol of the oxidized coenzyme per mol of protein (Table 1). Similar results were obtained with GDP-D-mannose as a substrate, suggesting that the enzymes containing bound NADPH also catalyze the initial dehydration reaction (results not shown). Preincubated GMDs, *i.e.* after all the coenzyme was converted to the oxidized form, were then subjected to dialysis followed by NADP$^+$ determination. No protein-associated coenzyme was detected after extensive dialysis (supplemental Figs. 1*C* and 2*C*). Conversely, dialysis of the untreated NADPH-containing GMD proteins had only slight effects on the content of both coenzyme forms. These results indicate that, whereas NADPH binds tightly to the viral GMDs, NADP$^+$ is easily dissociated from the proteins by dialysis. However, when untreated native ATCV-1 GMD was dialyzed, the NADP$^+$ already present in the protein remained bound to the protein. These results suggest that reduced coenzyme confers a different protein conformation that tightly binds the oxidized form. The putative guanylate species observed in the untreated native proteins were also present after dialysis, whereas they were completely removed after dialysis of the GDP-4-keto-6-deoxy-D-mannose-treated protein. This finding resembles the results reported for UDP-galactose 4-epimerase, where the NADPH-containing species has a significantly higher affinity for the substrate analogs (28). Preincubation of the proteins with GDP-4-keto-6-deoxy-D-mannose followed by extensive dialysis was then used to produce apoenzymes for the experiments described below.

Fluorescence Analysis—GMD fluorescent spectra were used to confirm the presence of bound NADPH and its oxidation to NADP$^+$ after incubation with GDP-4-keto-6-deoxy-D-mannose. Both PBCV-1 and ATCV-1 GMDs gave a strong emission with a maximum at ~440 and 443 nm, respectively, after excitation at 350 nm, thus confirming the presence of bound NADPH (Fig. 2*A*). The blue shift in emission wavelength of the protein-bound coenzyme compared with unbound NADPH (maximum, 455 nm), and the enhanced fluorescence agree with previous reports (19). Incubation of the two GMDs with GDP-4-keto-6-deoxy-D-mannose led to a complete disappearance of the fluorescence, confirming the oxidation of bound NADPH to NADP$^+$ (Fig. 2*A*). Similarly, fluorescence spectra of the purified apoGMDs had no emission around 440 nm (not shown).

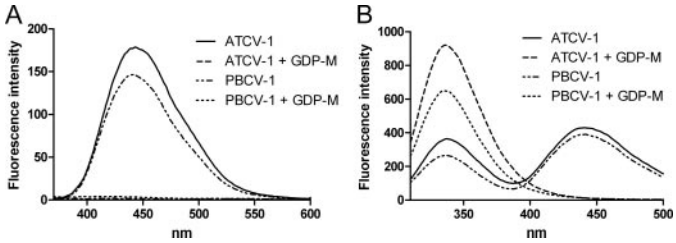

FIGURE 2. **Fluorescence emission spectra of native GMDs and GMDs incubated with GDP-4-keto-6-deoxy-D-mannose.** The final protein concentration was 1 μM in PBS. *A*, excitation was set at 350 nm. Native GMDs from both PBCV-1 and ATCV-1 had an emission spectrum with a maximum at 440 and 443 nm, respectively. Treatment of the proteins with GDP-4-keto-6-deoxy-D-mannose resulted in the loss of the fluorescence. *B*, excitation was set at 295 nm. Both proteins produced two emission peaks, with maxima at 336 and 440 nm for PBCV-1 GMD and 338 and 443 for ATCV-1 GMD, corresponding to emission of tryptophan and bound NADPH, respectively. GMD preincubated with GDP-4-keto-6-deoxy-D-mannose only had emission peaks at 336 and 338 nm, which displayed a highly increased fluorescence intensity.

Because amino acid sequence alignments indicated that GMD contains a well conserved tryptophan residue in close proximity to the active site (supplemental Fig. 3), we investigated the fluorescent properties of the native protein after excitation at 295 nm (Fig. 2*B*). Two emission peaks occurred; the first one corresponded to tryptophan emission with a maximum at 336–338 nm, whereas the second one had a maximum at about 440–443 nm, indicative of NADPH excitation by fluorescence energy transfer (29). When the enzymes were preincubated with GDP-4-keto-6-deoxy-D-mannose, the peak around 440 nm disappeared, and a significant increase in tryptophan fluorescence emission occurred at 336–338 nm (Fig. 2*B*). These results suggest that bound NADPH induces quenching of tryptophan fluorescence. When NADPH is oxidized to $NADP^+$ and the coenzyme is released from the protein, tryptophan quenching is lost. The emission spectrum of the purified apoenzyme with excitation at 295 nm was identical to that observed after treatment of the protein with GDP-4-keto-6-deoxy-D-mannose (results not shown).

Two methods, fluorescence enhancement of NADPH after binding to apoGMD and tryptophan fluorescence quenching were used to determine the NADPH and $NADP^+$ binding affinities (K_D), respectively, as reported previously for *E. coli* GMD and *Yersinia pseudotuberculosis* CDP-glucose 4,6-dehydratase (14, 19). ApoGMD was prepared by dialysis, as described above, and complete removal of the coenzymes was confirmed by HPLC. Fluorescence enhancement by NADPH binding to apoGMD is depicted in Fig. 3*A*. Analysis of the data by the Prism 5.0 program indicated that they best fit a one-site Hill binding equation. Apparent dissociation constant values of 0.71 ± 0.07 and 4.0 ± 0.2 μM were obtained for PBCV-1 and ATCV-1 GMDs, respectively. The Hill slope was 1.83 ± 0.35 for PBCV-1 GMD and 2.46 ± 0.19 for ATCV-1 GMD, suggesting cooperativity. Thus, these results indicate that PBCV-1 GMD has a higher affinity for NADPH than the ATCV-1 enzyme.

Titration of the apoGMDs with $NADP^+$ is reported in Fig. 3*B*. We observed quenching of protein fluorescence after correction for the inner filtering effect. However, higher concentrations of $NADP^+$ resulted in strong interference due to the high absorbance of the coenzyme at the excitation wavelength (295 nm). Using Equation 2 described under "Experimental

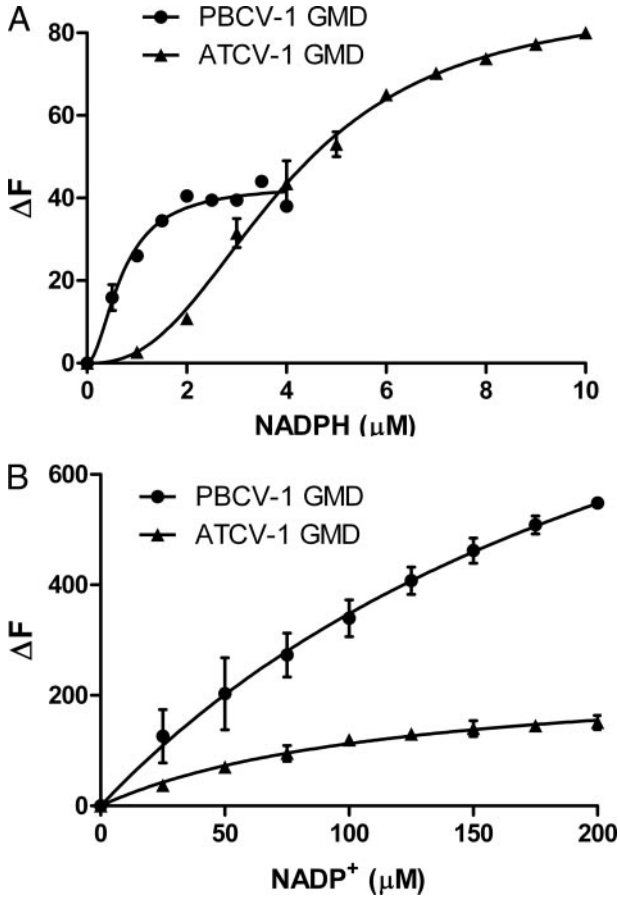

FIGURE 3. **Changes in fluorescence intensity during titration of apoGMDs with increasing concentrations of NADPH and $NADP^+$.** *A*, PBCV-1 and ATCV-1 apoGMDs were diluted to 0.5 μM in PBS and titrated with increasing concentration of NADPH. The excitation wavelength was set at 350 nm. ΔF was obtained by subtracting the fluorescence intensity of NADPH solutions of the same concentration used for titration from the fluorescence intensity of the samples containing the protein. *B*, PBCV-1 and ATCV-1 apoGMDs were diluted to 0.5 μM in PBS and titrated with $NADP^+$. ΔF was derived by subtraction of the fluorescence intensity of the protein with the added ligand from the intensity of the protein solution without any added $NADP^+$.

Procedures," a ΔF_{max} of 249 ± 20 with an apparent K_D of 121 ± 20 μM was calculated for ATCV-1 GMD. However, it was not possible to calculate a $NADP^+$ K_D for the PBCV-1 enzyme. Thus, the results confirm that the viral GMDs, and in particular the PBCV-1 enzyme, have a very low affinity for $NADP^+$.

Size Exclusion Chromatography—The role of coenzyme binding on the structural properties of PBCV-1 and ATCV-1 GMDs was examined by SEC. SEC of the PBCV-1-purified active enzyme indicated that native PBCV-1 GMD elutes with an apparent molecular mass of 87 kDa, suggesting a dimeric structure in solution (Fig. 4*A*). To exclude any influence of protein conformation on the apparent molecular mass of PBCV-1 GMD (30), we conducted a parallel SEC analysis of GMD/MUR1 from *A. thaliana*. Overall, the *A. thaliana* enzyme has the same protein crystal structure (15, 17) as the PBCV-1 enzyme and was expected to have elution properties similar to PBCV-1 GMD. The results obtained with the *A. thaliana* enzyme indicated a mass of ~160 kDa,[3] corresponding to the tetrameric form observed by x-ray crystallography (15). A further demonstration of the oligomeric structure of PBCV-1 GMD in solution was obtained by BS^3 (bis(sulfosuccinimid-

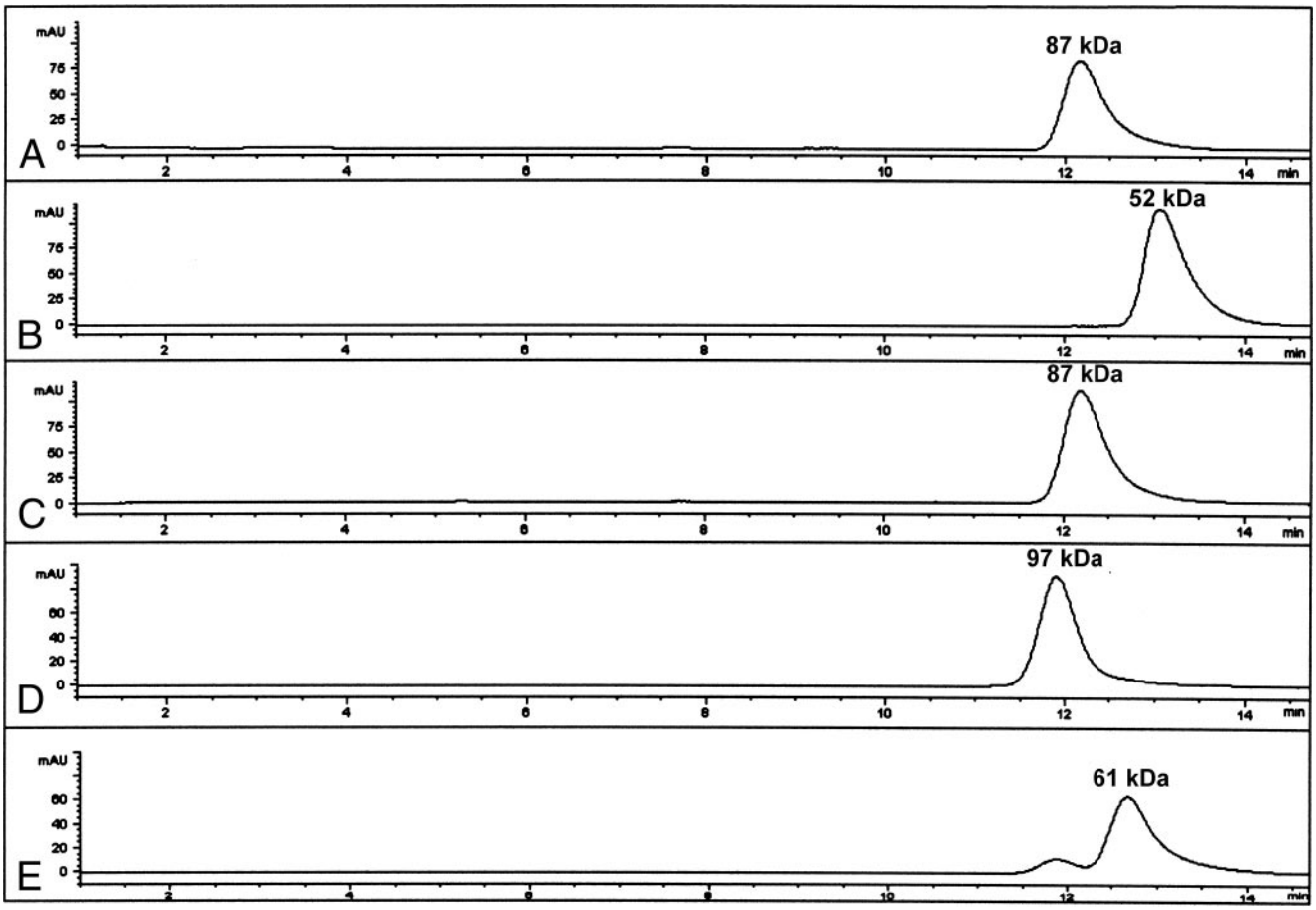

FIGURE 4. **Size exclusion chromatography of native and treated GMDs.** *A*, native PBCV-1 GMD (5 μM). *B*, purified PBCV-1 apoGMD (5 μM). *C*, purified PBCV-1 apoGMD (5 μM) incubated in the presence of NADPH (10 μM). *D*, native ATCV-1 GMD (5 μM). *E*, native ATCV-1 GMD incubated with molar excess of GDP-4-keto-6-deoxy-D-mannose and kept at 4 °C for 24 h. *mAU*, milliabsorbance units. *mAU*, milliabsorbance units.

yl)suberate) cross-linking experiments of the native protein followed by SDS-PAGE, as previously performed with human GMD (31). The results revealed a main band migrating slightly higher than the 75-kDa standard (results not shown), consistent with a dimeric structure.

To evaluate the structural effects of converting NADPH to $NADP^+$, 5 μM PBCV-1 GMD was incubated with GDP-4-keto-6-deoxy-D-mannose and immediately subjected to SEC analysis. The dimeric form was converted to a form with a higher elution time, which was proportional to the amount of added GDP-4-keto-6-deoxy-D-mannose. The new elution time was observed also for the purified apoenzyme, which exhibited an apparent mass of 52 kDa (Fig. 4*B*). This is higher than the expected mass of the monomer (40 kDa), but it is compatible with loss of the quaternary structure.

To determine whether the addition of coenzymes restores the PBCV-1 GMD dimeric form, apoGMD was incubated with increasing concentrations of either NADPH or $NADP^+$. NADPH addition led to complete conversion of the monomeric to the dimeric form, already at low coenzyme concentrations (Fig. 4*C*). In contrast, no dimerization occurred when $NADP^+$ was added, even at millimolar concentrations. A progressive decrease in the peak area corresponding to the monomer occurred when $NADP^+$ concentrations were higher than 5 mM (results not shown). A likely explanation is that the protein aggregates in high concentrations of $NADP^+$, which either precipitates out of solution or is retained on the column.

A similar elution behavior was observed for ATCV-1 GMD. The protein containing both $NADP^+$ and NADPH eluted as a single peak, with an apparent molecular mass of 97 kDa (Fig. 4*D*). After incubation with GDP-4-keto-6-deoxy-D-mannose to convert NADPH to $NADP^+$, the elution time of the protein (at 5 μM concentration) immediately after pretreatment was identical to that of untreated GMD (results not shown). If the treated GMD was either diluted further or maintained at 4 °C for 24 h, a new peak formed with an apparent molecular mass of 61 kDa (Fig. 4*E*). Like PBCV-1, ATCV-1 apoenzyme eluted with the same retention time as the new peak (not shown). Similarly to PBCV-1 GMD, incubation with increasing concentrations of NADPH restored the dimeric form at 97 kDa (not shown). Concentrations of $NADP^+$ higher than 50 μM also promoted partial formation of the dimer, at variance with the results from the PBCV-1 enzyme; however, complete dimerization of the ATCV-1 enzyme never occurred with only $NADP^+$ (results not shown). Like PBCV-1 GMD, a loss of the ATCV-1 protein occurred, probably as aggregation, when $NADP^+$ was added at millimolar concentrations.

Enzymatic Activities—PBCV-1 and ATCV-1 GMD dehydratase and reductase activities are reported in Table 2. When incubated in the presence of 100 μM GDP-4-keto-6-deoxy-D-

TABLE 2

Specific activity of GMD from PBCV-1 and ATCV-1 viruses

Specific activity was determined using 100 μM ^{14}C-labeled GDP-D-mannose or GDP-4-keto-6-deoxy-D-mannose as substrates for dehydratase and reductase activities, respectively. Product formation was determined by reverse phase HPLC analysis followed by continuous flow scintillation counting. ND, not detected.

	Specific activity	
	PBCV-1 GMD	ATCV-1 GMD
	μmol/h/mg of protein	
Dehydratase activity	28.6 ± 8.3	37.6 ± 7.3
Reductase activity	510.3 ± 15.7	ND

mannose and exogenously added NADPH, PBCV-1 GMD had a high reductase activity, which is 1 order of magnitude higher than the dehydratase activity. As predicted, the putative ATCV-1 GMD had dehydratase activity with GDP-D-mannose. However, no reductase activity was detected with the ATCV-1 GMD, which is similar to other GMDs. This finding indicates that, even if the ATCV-1 enzyme is able to use the bound NADPH to reduce GDP-4-keto-6-deoxy-D-mannose, it is not able to exchange the bound $NADP^+$ with the exogenous NADPH, which is essential to perform the reductase activity.

GMD activity was also measured after pretreatment of the concentrated protein (100 μM) with GDP-4-keto-6-deoxy-D-mannose (150 μM) to induce conversion of NADPH to $NADP^+$. Pretreatment of PBCV-1 GMD led to an immediate and complete loss of dehydratase activity in all conditions tested. In contrast, pretreatment of ATCV-1 GMD, which completely converted bound NADPH to $NADP^+$, resulted in an approximate 1.5-fold increase in dehydratase activity when the protein was tested immediately after pretreatment with the GDP-4-keto-6-deoxy-D-mannose. If the pretreated protein was kept at a low concentration (5 μM), it lost activity in 24 h, whereas the native ATCV-1 GMD retained activity. When both native and pretreated proteins were kept at 4 °C at high concentration (100 μM), a progressive decrease (over several weeks) in the specific activity occurred that was always faster for the pretreated protein.

After demonstrating that native recombinant PBCV-1 GMD only binds NADPH and that conversion of NADPH to $NADP^+$ results in complete inactivation of the enzyme, the effects of these two coenzymes were investigated using the apoenzyme. As previously reported for *E. coli* GMD (14) and *Y. pseudotuberculosis* CDP-D-glucose 4,6-dehydratase (19), the apoGMD was intrinsically inactive. We then incubated either 0.5 μM PBCV-1 native GMD or apoGMD and 50 μM GDP-D-mannose with increasing amounts of $NADP^+$ or NADPH. Both $NADP^+$ and NADPH significantly increased native GMD activity (Fig. 5), confirming previous results with the PBCV-1 enzyme (9). The addition of micromolar concentrations of NADPH to apoGMD reactivated the enzyme, resulting in the synthesis of both GDP-4-keto-6-deoxy-D-mannose and GDP-D-rhamnose (directly proportional to the amount of NADPH added), due to the combination of both dehydratase and reductase activities (Fig. 5*A*). In contrast, dehydratase activity only occurred when $NADP^+$ concentrations were higher than 0.5 mM (Fig. 5*B*).

Activity of the ATCV-1 apoenzyme with either NADPH or $NADP^+$ using 100 μM GDP-D-mannose as substrate is reported in Fig. 6. Like the PBCV-1 enzyme, NADPH alone reactivated the ATCV-1 apoenzyme (Fig. 6*A*). However, unlike PBCV-1

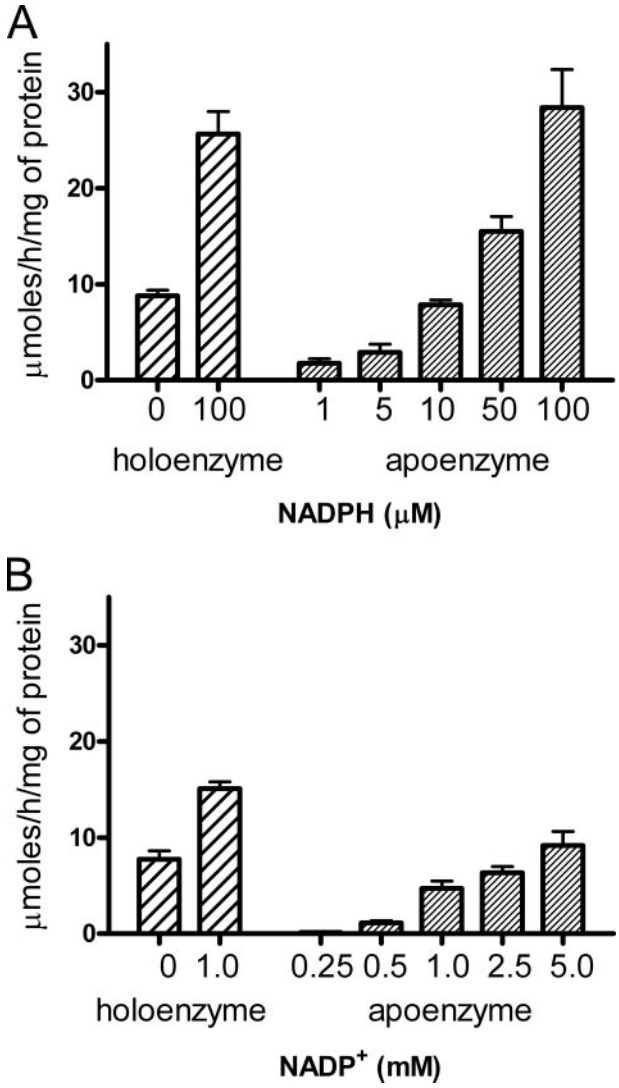

FIGURE 5. **Effects of $NADP^+$ and NADPH on PBCV-1 apoGMD enzyme activity.** The enzyme activities of native GMD and apoGMD (both 0.5 μM) were determined with 50 μM GDP-D-mannose as substrate. *A*, holoenzyme and apoenzyme were incubated with increasing concentrations of NADPH. Activity was expressed as the rate of disappearance of the substrate GDP-D-mannose as determined by HPLC analysis because both GDP-4-keto-6-deoxy-D-mannose and GDP-D-rhamnose (directly proportional to the amount of added NADPH) were produced. *B*, native GMD or the apoGMD were incubated with increasing concentrations of $NADP^+$. Apoenzyme alone had no activity.

GMD, no GDP-D-rhamnose formed, confirming that ATCV-1 GMD has no reductase activity. $NADP^+$ also reactivated the apoenzyme but at much higher concentrations than NADPH, with a maximum at 0.5 mM. Additional increases in $NADP^+$ resulted in loss of enzymatic activity (Fig. 6*B*).

Phylogenetic Analyses—Maximum parsimony (heuristic), neighbor joining (distance method), and maximum parsimony using bootstrap (1000 replicates) analyses produced very similar tree topologies. The GMD phylogram shown in Fig. 7 was constructed using the bootstrap algorithm in PAUP (27). PBCV-1 GMD is the most evolutionary diverged of the taxa in the tree. The long length of the horizontal lines in the tree and the fact that PBCV-1 GMD is not a member of a clade indicate extensive evolutionary divergence, whereas the ATCV-1 GMD falls in a clade of bacterial GMDs. In contrast, the GMER tree

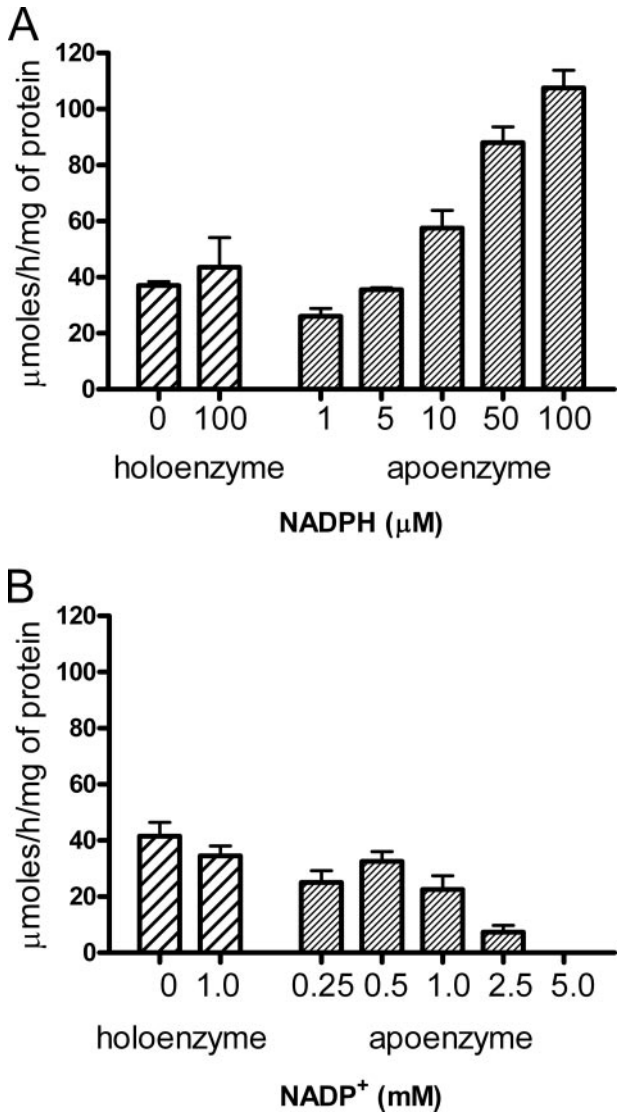

FIGURE 6. **Effects of $NADP^+$ and NADPH on ATCV-1 apoGMD activity.** The enzyme activities of native GMD and apoGMD (both 0.5 μM) were determined with 100 μM GDP-D-mannose as substrate. *A*, holoenzyme and apoenzyme were incubated with increasing concentrations of NADPH. Activity was expressed as the rate of GDP-4-keto-6-deoxy-D-mannose formation determined by HPLC analysis. GDP-D-rhamnose was not detected in these conditions. *B*, native GMD or apoGMD was incubated with increasing concentrations of $NADP^+$. No activity was observed for the apoenzyme without adding coenzyme.

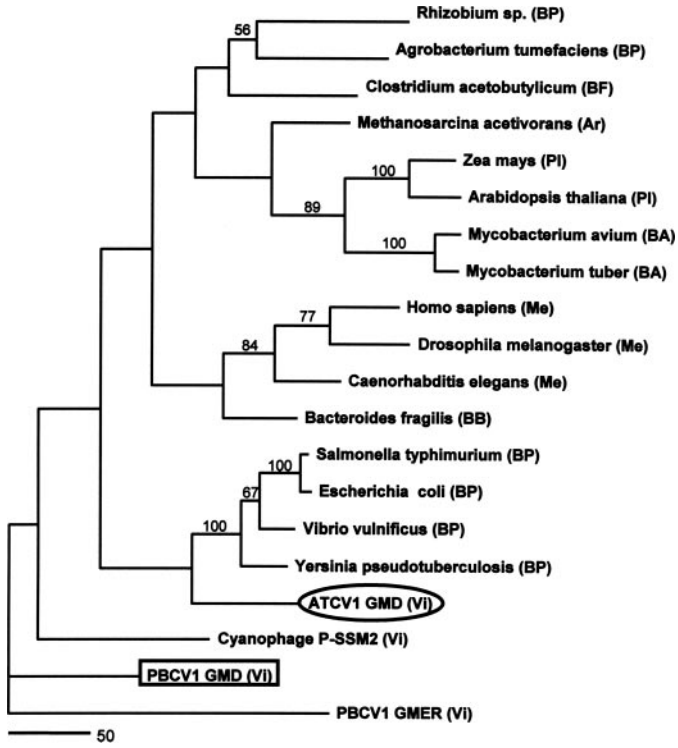

FIGURE 7. **Rooted phylogram of GMD.** A BLAST search was conducted using the virus PBCV-1 GMD protein (PBCV-1: AAC96486). The sequence for ATCV-1 (*A. turfacea* chlorella virus) GMD is open reading frame Z804L in accession number EF101928. The sequence for PBCV-1) (AAC96663) was used as the out-group in the phylogenetic analyses. ClustalW was used to align the sequences. Bootstrap analysis (heuristic using parsimony) was used to construct the tree. Similar tree topologies were produced by neighbor joining and maximum parsimony analyses. The values on the branches are the percentage of bootstrap support (1000 replicates). Only bootstrap values >50% are shown. BA, bacteria Actinobacteria; *BB*, bacteria Bacteroidetes; *BF*, bacteria Firmicutes; *BP*, bacteria Proteobacteria; *Ar*, Archaea; *Me*, Metazoa; *Pl*, plants; *Vi*, double-stranded DNA virus. Accession numbers are as follows: *Agrobacterium tumefaciens* strain C58 (AAL45583); *A. thaliana* (AAF07199); *Bacteroides fragilis* (AAL61891); *Caenorhabditis elegans* (CAC42270); *Clostridium acetobutylicum* (AAK80138); *Cyanophage* P-SSM2 (YP_214488); *Drosophila melanogaster* (AAL90257); *E. coli* (1DB3); *Homo sapiens* (AAC13553); *Methanosarcina acetivorans* strain C2A (AAM04594); *Mycobacterium avium* (AAD20373); *Mycobacterium tuberculosis* CDC155 (AAK45828); *Rhizobium sp.* NGR234 (AAB91604); *Salmonella typhimurium* (AAG24813); *Vibrio vulnificus* (NP_933142); *Y. pseudotuberculosis* (ZP_00794554); *Zea mays* (AAF70818).

(supplemental Fig. 4) indicates that PBCV-1 and ATCV-1 GMERs are more similar to one another (same clade) than to other taxa in the analysis.

DISCUSSION

GMD is a widely represented enzyme in all taxa, from bacteria to animals and plants. Recently, GMD-encoding genes were identified in a few viruses, such as the chlorella viruses reported in this paper and a cyanophage P-SSM2 infecting *Prochlorococcus* cyanobacteria (32). GMD is involved in the first step of the *de novo* biosynthesis of GDP-L-fucose, the donor substrate for fucosyltransferase activity. Fucose is found in many glycoconjugates of prokaryotes and eukaryotes, where it often plays a fundamental role in cell-cell adhesion and recognition (33). Genes encoding the second enzyme in the pathway, GMER, were also identified in the chlorella viruses and in cyanophage P-SSM2, suggesting that the synthesis of GDP-L-fucose plays an important role in their life cycles, but this is unknown at the present time. Interestingly, all these viruses infect photosynthetic organisms.

The presence of a tightly bound $NADP^+$ is essential for the proposed catalytic activity of GMD (34, 35), as demonstrated by the complete loss of activity by the apoenzyme (14). However, recent GMD crystal structures at 2.2 Å resolution from *A. thaliana* and *P. aeruginosa* indicate unambiguously the presence of NADPH, and not $NADP^+$, bound to the proteins (15–16). Unfortunately, the low resolution of the PBCV-1 structure did not allow the oxidized and reduced forms of the coenzyme to be distinguished (17). Likewise, the reduced coenzyme NADH was present in recombinant CDP-D-glucose 4,6-dehydratase (19). The occurrence of NADH together with NAD^+ has also been reported for UDP-glucose 4-epimerase and dTDP-D-glucose 4,6-dehydratase, suggesting that a bound reduced coenzyme is a common feature of many enzymes in the reductase-epime-

rase-dehydrogenase superfamily (28, 36). Crystal structures of some of these enzymes have been obtained with the oxidized coenzyme, NAD^+ (37–39), whereas in the case of GMDs, crystals were obtained either without any coenzyme or with only bound NADPH (14–16).

The presence of NAD(P)H is not completely surprising, since these enzymes have a higher affinity for the reduced form of the coenzyme, as compared with $NAD(P)^+$ (14, 19). In fact, the high affinity of the enzymes for NAD(P)H could prevent its dissociation during the catalytic cycle, when the hydride is transiently transferred from sugar C-4 to the coenzyme. However, in all these reports, the NAD(P)H-containing enzymes have been viewed as abortive forms, devoid of enzymatic activity (28, 36).

Analysis of dinucleotide content in freshly purified recombinant viral GMDs revealed variable ratios of $NADP^+$ to NADPH for the ATCV-1 enzyme and only NADPH for the PBCV-1 protein. It is possible that, under the expression conditions of the recombinant proteins, most of the protein molecules bind NADPH instead of $NADP^+$, and this confers a more stable conformation. If the NADPH-containing protein is viewed as an abortive form, oxidation of NADPH to $NADP^+$ should result in the recovery of enzymatic activity. Indeed, oxidation of NADPH in ATCV-1 GMD led to an initial increase in the enzyme specific activity but only when the enzyme was kept at high concentrations and for a short time. In contrast, NADPH oxidation of PBCV-1 GMD resulted in a complete and immediate loss of the dehydratase activity. The loss of the enzymatic activity for both enzymes was accompanied by release of the bound oxidized coenzyme and conversion of the dimeric structure to a monomeric form. Thus, the data reported here indicate that viral GMDs in solution not only contain NADPH but that NADPH is essential for protein structure and activity. These results were confirmed by the experiments with the apoenzymes, which establish that NADPH is more efficient in restoring both structure and enzymatic activity of the viral GMDs. Furthermore, the results indicate that $NADP^+$ alone does not promote subunit dimerization but that it induces aggregation or precipitation of the proteins when used at millimolar concentrations. Thus, the correct conformation of the apoenzyme probably does not occur with only $NADP^+$.

When PBCV-1 and ATCV-1 recombinant GMDs were maintained at 4 °C for several weeks, we observed a gradual loss in NADPH content. This loss might be due to oxidation, which occurred faster for the ATCV-1 enzyme and which paralleled a decrease in its enzymatic activity and conversion of its dimeric form to the monomeric form.[3] Thus, oxidation of bound NADPH could explain the intrinsic instability reported for several GMDs (2, 31). Oxidation of NADPH by the product of the dehydration reaction could also provide a mechanism to control the activity of the whole GDP-L-fucose pathway. In fact, *in vivo* the intermediate GDP-4-keto-6-deoxy-D-mannose is immediately converted to the final product GDP-L-fucose by the GMER enzyme. GDP-L-fucose is then responsible for feedback inhibition of GMD (7, 31). If GMER activity does not remove the intermediate compound efficiently, GDP-4-keto-6-deoxy-D-mannose accumulation could result in destabilization of GMD, thus blocking GDP-D-mannose consumption, an essential metabolite for all glycosylation processes. Co-expression of *A. thaliana* MUR1/GMD with its corresponding GMER resulted in GMD stabilization and increased dehydratase activity; however, in this report a direct interaction between the two enzymes was postulated (40). Studies on the functional properties of eukaryotic GMDs are currently in progress to test this hypothesis. Indeed, preliminary data on human GMD indicates the presence of both tightly bound $NADP^+$ and NADPH as well as incubation of the protein with the intermediate compound induced oxidation of the bound coenzyme, similar to the data reported in this study.[3] Interestingly, results reported for recombinant human and *E. coli* GMDs showed severalfold increases in enzymatic activity when micromolar concentrations of NADPH were added, suggesting that NADPH also plays an important role in the bacterial and eukaryotic enzymes (7).

The presence of one $NADP^+$ and one NADPH in each functional dimer of ATCV-1 GMD is compatible with the proposed catalytic mechanism such that $NADP^+$ is essential for enzymatic activity, whereas NADPH is essential for stabilizing the protein structure. However, the PBCV-1 GMD differs significantly from the ATCV-1 GMD because the purified PBCV-1 recombinant enzyme contains tightly bound NADPH and $NADP^+$ is only present in trace amounts in freshly purified protein. In this condition the protein displays full enzymatic activity. Binding of NADPH instead of $NADP^+$ to purified PBCV-1 GMD raises questions about its catalytic mechanism, since the only proposed mechanism requires the presence of an oxidized coenzyme. At present, we do not have an explanation for this finding nor are we able to propose an alternative mechanism. Furthermore, the low resolution of PBCV-1 x-ray structure does not provide any clues to explain this finding. However, GMD amino acid alignments reveal some differences in conserved stretches of amino acids, which are in close proximity to the active site; these differences only occur in the PBCV-1 enzyme. Thus, at least some of these amino acid substitutions (in particular several cysteine residues, highlighted in GMD alignment in supplemental Fig. 3) are undoubtedly responsible for the differences observed between GMD from PBCV-1 and those from the other. Direct comparisons of the properties between the virus GMDs and GMDs from other organs as well as currently ongoing site-directed mutagenesis experiments should provide an explanation for this issue and also for the high reductase activity, leading to GDP-D-rhamnose formation, displayed by only the PBCV-1 enzyme.

The different affinities for $NADP^+$/NADPH by the ATCV-1 and PBCV-1 GMDs could in part explain the different enzymatic properties between the two proteins. In fact, the extremely low affinity of the PBCV-1 enzyme for $NADP^+$ together with a high affinity for NADPH could lead to NADPH replacing $NADP^+$. This replacement could explain the high reductase activity by the PBCV-1 enzyme. In contrast, this replacement probably does not occur for the ATCV-1 enzyme, which has a lower affinity toward NADPH and higher affinity toward $NADP^+$ compared with the PBCV-1 GMD. This difference could explain the lack of reductase activity.

The unusual catalytic behavior of PBCV-1 GMD compared with ATCV-1 is also reflected in amino acid sequence differences. ATCV-1 GMD is more similar to GMDs from other organisms than it is to PBCV-1 GMD. For example, ATCV-1 and

PBCV-1 GMDs have 66 and 56% identity with the *Yersinia enterocolitica* enzyme, respectively, whereas the identity between the two viral enzymes is only 53%. This difference is also reflected in the phylogenic analyses, which indicates that PBCV-1 GMD is the most evolutionarily diverged of the GMDs, whereas ATCV-1 GMD clusters with bacterial GMDs.

The phylogenetic analyses help form hypotheses about past evolutionary events. One hypothesis is that PBCV-1 GMD is older than ATCV-1 GMD, which would indicate that the two viruses acquired their GMDs by separate events in evolutionary time. If this hypothesis is correct, then it is difficult to explain why GMER, which completes the second step in the pathway from mannose to fucose, is so similar for the two viruses (supplemental Fig. 4). A second hypothesis, and one we favor, is that both GMD and GMER genes were acquired by the ancestor of PBCV-1 and ATCV-1 before their divergence. The high degree of similarity between the PBCV-1 and ATCV-1 GMERs (supplemental Fig. 4) supports this hypothesis. We propose that the high degree of evolutionary divergence between PBCV-1 and ATCV-1 GMDs occurred because the former evolved a second enzymatic function after the divergence of the PBCV-1 and ATCV-1 viruses from their common ancestor. PBCV-1 GMD evolved faster than ATCV-1 GMD because it faced two evolutionary pressures, one to remain as a functional dehydratase (continue as an ortholog) and the second to become a new reductase (become a new paralog that could synthesize rhamnose). It is the second evolutionary pressure that would have required many amino acid substitutions in PBCV-1 GMD, as compared with ATCV-1 GMD that did not evolve new reductase activity. In fact, accumulating evidence indicates that the chlorella viruses, including PBCV-1 and ATCV-1, have a long evolutionary history (41), possibly dating back to the time that prokaryotic and eukaryotic organisms separated, ~2.0–2.7 billion years ago (42–45). Although we do not have an estimate of the time since the divergence of the PBCV-1 and ATCV-1 viruses, there was likely enough time, particularly when considering the short life cycle of a virus, to allow for the evolution of reductase activity in PBCV-1 GMD.

REFERENCES

1. Tonetti, M., Sturla, L., Bisso, A., Zanardi, D., Benatti, U., and De Flora, A. (1998) *Biochimie* (*Paris*) **80,** 923–931.
2. Kneidinger, B., Graninger, M., Adam, G., Puchberger, M., Kosma, P., Zayni, S., and Messner, P. (2001) *J. Biol. Chem.* **276,** 5577–5583
3. Maki, M., Jarvinen, N., Rabina, J., Maaheimo, H., Mattila, P., and Renkonen, R. (2003) *Glycobiology* **13,** 295–303.
4. Albelmann, C., and Piepersberg, W. (2001) *Glycobiology* **11,** 655–661
5. Bonin, C. P., Potter, I., Vanzin, G. F., and Reiter, W.-D. (1997) *Proc. Natl. Acad. Sci. U. S. A.* **94,** 2085–2090
6. Sturla, L., Bisso, A., Zanardi, D., Benatti, U., De Flora, A., and Tonetti, M. (1997) *FEBS Lett.* **412,** 126–130
7. Sullivan, F. X., Kumar, R., Kriz, R., Stahl, M., Xu, G., Rouse, J., Chang, X., Boodhoo, A., Potvin, B., and Cumming, D. A. (1998) *J. Biol. Chem.* **273,** 8193–8202
8. Wu, B., Zhang, Y., and Wang, P. G. (2001) *Biochem. Biophys. Res. Commun.* **285,** 364–371
9. Tonetti, M., Zanardi, D., Gurnon, J., Fruscione, F., Armirotti, A., Damonte, G., Sturla, L., De Flora, A., and Van Etten, J. L. (2003) *J. Biol. Chem.* **278,** 21559–21565
10. Van Etten, J. L. (2003) *Annu. Rev. Genet.* **37,** 153–195
11. Graves, M. V., Bernadt, C. V., Cerny, R., and Van Etten, J. L. (2001) *Virology* **285,** 332–345
12. Kallberg, Y., Oppermann, U., Jornvall, H., and Persson, B. (2002) *Protein Sci.* **11,** 636–641
13. Labesse, G., Vidal-Cros, A., Chomilier, J., Gaudry, M., and Mornon, J.-P. (1994) *Biochem. J.* **304,** 95–99
14. Somoza, J. R., Menon, S., Schimdt, H., Joseph-McCarthy, D., Dessen, A., Stahl, M. L., Somers, W. S., and Sullivan, F. X. (2000) *Structure* **8,** 123–135
15. Mulichak, A. M., Bonin, C. P., Reiter, W.-D., and Garavito, R. M. (2002) *Biochemistry* **41,** 15578–15589
16. Webb, N. A., Mulichack, A. M., Lam, J. S., Rocchetta, H. L., and Garavito, R. M. (2004) *Protein Sci.* **13,** 529–539
17. Rosano, C., Zuccotti, S., Sturla, L., Fruscione, F., Tonetti, M., and Bolognesi, M. (2006) *Biochem. Biophys. Res. Commun.* **339,** 191–195
18. Hegeman, A. D., Gross, J. W., and Frey, P. A. (2001) *Biochemistry* **40,** 6598–6610
19. He, X., Thorson, J. S., and Liu, H. (1996) *Biochemistry* **35,** 4721–4731
20. Fitzgerald, L. A., Graves, M. V., Li, X., Hartigan, J., Pfitzner, A. J., Hoffart, E., and Van Etten, J. L. (2007) *Virology* **362,** 350–361
21. Gasteiger, E., Hoogland, C., Gattiker, A., Duvaud, S., Wilkins, M. R., Appel, R. D., and Bairoch, A. (2005) in *The Proteomics Protocols Handbook* (Walker, J. M., ed) pp. 571–607, Humana Press Inc., Totowa, NJ
22. Lowry, O. H., Passonneau, J. V., and Rock, M. K. (1961) *J. Biol. Chem.* **236,** 2756–2759
23. McCracken, J. A., Wang, L., and Kohen, A. (2004) *Anal. Biochem.* **324,** 131–136
24. Lakowics, J. R. (1983) *Principles of Fluorescence Spectroscopy*, p. 44, Plenum Press, New York
25. Welling, G. W., and Welling-Wester, S. (1989) in *HPLC of Macromolecules: A Practical Approach* (Oliver, R.W., ed) pp. 77–89, Oxford University Press, Oxford
26. Tonetti, M., Sturla, L., Bisso, A., Benatti, U., and De Flora, A. (1996) *J. Biol. Chem.* **271,** 27274–27279
27. Swafford, D. L. (2000) *PAUP*. Phylogenetic Analysis with Parsimony* (**and Other Methods*) Version 4.10, Sinauer Associates, Sunderland, MA
28. Vanhooke, J. L., and Frey, P. A. (1994) *J. Biol. Chem.* **269,** 31496–31504
29. Li, B., and Lin, S. (1996) *Eur. J. Biochem.* **235,** 180–186
30. Goetz, H., Kuschel, M., Wulff, T., Sauber, C., Miller, C., Fisher, S., and Woodward, C. (2004) *J. Biochem. Biophys. Methods* **60,** 281–293
31. Bisso, A., Sturla, L., Zanardi, D., De Flora, A., and Tonetti, M. (1999) *FEBS Lett.* **456,** 370–374
32. Sullivan, M. B., Coleman, M.-L., Weigele, P., Rower, F., and Chisholm, S. W. (2005) *PLoS Biol.* **3,** e144
33. Ma, B., Simala-Grant, J. C., and Taylor, D. E. (2006) *Glycobiology* **16,** 158–184
34. Allard, S. T. M., Beis, K., Giraud, M., Hegeman, A. D., Gross, J.-W., Wilmouth, R. C., Whitfield, C., Graniger, M., Messner, P., Allen, A. G., Maskell, D. J., and Naismith, J. H. (2002) *Structure* **10,** 81–92
35. Oths, P. J., Mayer, R. M., and Floss, H. G. (1990) *Carbohydr. Res.* **198,** 91–100
36. Beis, K., Allard, S. T. M., Hegeman, A. D., Murshudov, G., Philp, D., and Naismith, J. H. (2003) *J. Am. Chem. Soc.* **125,** 11872–11878
37. Allard, S. T., Giraud, M. F., Whithfield, C., Graniger, M., Messner, P., and Naismith, J. H. (2001) *J. Mol. Biol.* **307,** 283–295
38. Vogan, E. M., Bellamacina, C., He, X., Liu, H., Ringe, D., and Petsko, G. A. (2004) *Biochemistry* **43,** 3057–3067
39. Thoden, J. B., Frey, P. A., and Holden, H. M., (1996) *Biochemistry* **35,** 2557–2566
40. Nakayama, K., Maeda, Y., and Jigami, Y. (2003) *Glycobiology* **13,** 673–680
41. Dunigan, D. D., Fitzgerald, L. A., and Van Etten, J. L. (2006) *Virus Res.* **117,** 119–132
42. Han, T. M., and Runnegar, B. (1992) *Science* **257,** 232–235
43. Feng, D. G., Cho, G., and Doolittle, R. F. (1997) *Proc. Natl. Acad. Sci. U. S. A.* **94,** 13028–13033
44. Brocks, J. J., Logan, G. A., Buick, R., and Summons, R. E. (1999) *Science* **285,** 1033–1036
45. Glansdorff, N. (2000) *Mol. Microbiol.* **38,** 177–185

Differential Role of $NADP^+$ and NADPH in the Activity and Structure of GDP-D-mannose 4,6-Dehydratase from Two Chlorella Viruses

Floriana Fruscione, Laura Sturla, Garry Duncan, James L. Van Etten, Paola Valbuzzi, Antonio De Flora, Eleonora Di Zanni and Michela Tonetti

J. Biol. Chem. 2008, 283:184-193.
doi: 10.1074/jbc.M706614200 originally published online November 1, 2007

Legends to figures (Supplemental data)

Figure 1. HPLC analysis of the coenzymes bound to PBCV-1 GMD. (A) Native protein extracted with NaOH to determine bound NADPH. (B) Native protein extracted with perchloric acid to determine bound $NADP^+$. (C) Apo-GMD obtained after treatment with GDP-4-keto-6-deoxy-D-mannose and dialysis, followed by perchloric acid extraction. Arrows indicate the elution time of standard $NADP^+$ and NADPH. Letter G denotes peaks that exhibit a guanylate spectrum.

Figure 2. HPLC analysis of the coenzymes bound to ATCV-1 GMD. (A) Freshly purified GMD extracted with NaOH to determine bound NADPH. (B) Freshly purified GMD extracted with perchloric acid to determine bound $NADP^+$. (C) Apo-GMD obtained after treatment with GDP-4-keto-6-deoxy-D-mannose and dialysis, followed by perchloric acid extraction. Arrows indicate the elution time of standard $NADP^+$ and NADPH. Letter G denotes peaks that exhibit a guanylate spectrum.

Figure 3. Sequence alignment of GMDs. ClustalW was used to align the sequences of ATCV-1, PBCV-1 (AAC96486), *H. sapiens* (AAC13553), *E. coli* (1DB3A) and *A. thaliana* (mur1, P93031) GMDs. Box indicates the GXXGXXG motif involved in coenzyme binding. Arrows indicate the residues involved in the catalytic mechanism. Cysteine residues, which are present in PBCV-1 GMD only and which are in close proximity to the active site, are highlighted in jellow.

Figure 4. **Rooted phylogram of GDP-4-keto-6-deoxy-D-mannose epimerase/reductase (GMER).** A BLAST was conducted using the GMER gene of PBCV-1: AAC96663. The sequence for ATCV-1 GMER corresponds to ORF Z282L in GenBank accession number EF101928. The sequence for GDP-D-mannose dehydratase (GMD) (AAC96486) was used as the outgroup in the phylogenetic analyses.ClustalW was used to align the sequences. Maximum parsimony was used to construct the tree. Similar tree topologies were produced by neighbor joining and bootstrap analyses. The values on the branches are the percentage of bootstrap support (1000 replicates). Only bootstrap values > 50% are shown. Key: BA = Bacteria Actinobacteria**;** BB = Bacteria Bacteroidetes; BF = Bacteria Firmicutes; BP = Bacteria Proteobacteria; BT = Bacteria Thermotogae; Ar = Archaea; Me = Metazoa; Pl = Plants; Vi = dsDNA virus. Accession numbers are as follows: *Agrobacterium tumefaciens* str. C58 (AAK88659); *Azorhizobium caulinodans* (AAB24744); *Bacteroides fragilis* (AAL61890); *Bradyrhizobium* sp. WM9 (AAK00171); *Caenorhabditis elegans* (AAA50647); *Campylobacter jejuni* (CAB73852); *Clostridium acetobutylicum* (AAK80137); *Drosophila melanogaster* (AAF46924); *Escherichia coli1E6U* (1E6U); *Homo sapiens* (AAC50786); *Laminaria digitata* (CAB61336); *Methanococcus jannaschii* (AAB98196); *Methanosarcina acetivorans* (AAM04606); *Mycobacterium tuberculosis* (AAK45829); *Pyrococcus furiosus* (AAL81912); *Salmonella typhimurium* (AAL21012); *Thermotoga maritima* (AAD35594); *Vibrio cholerae* (BAA33627).

Figure 1 –Supplemental data

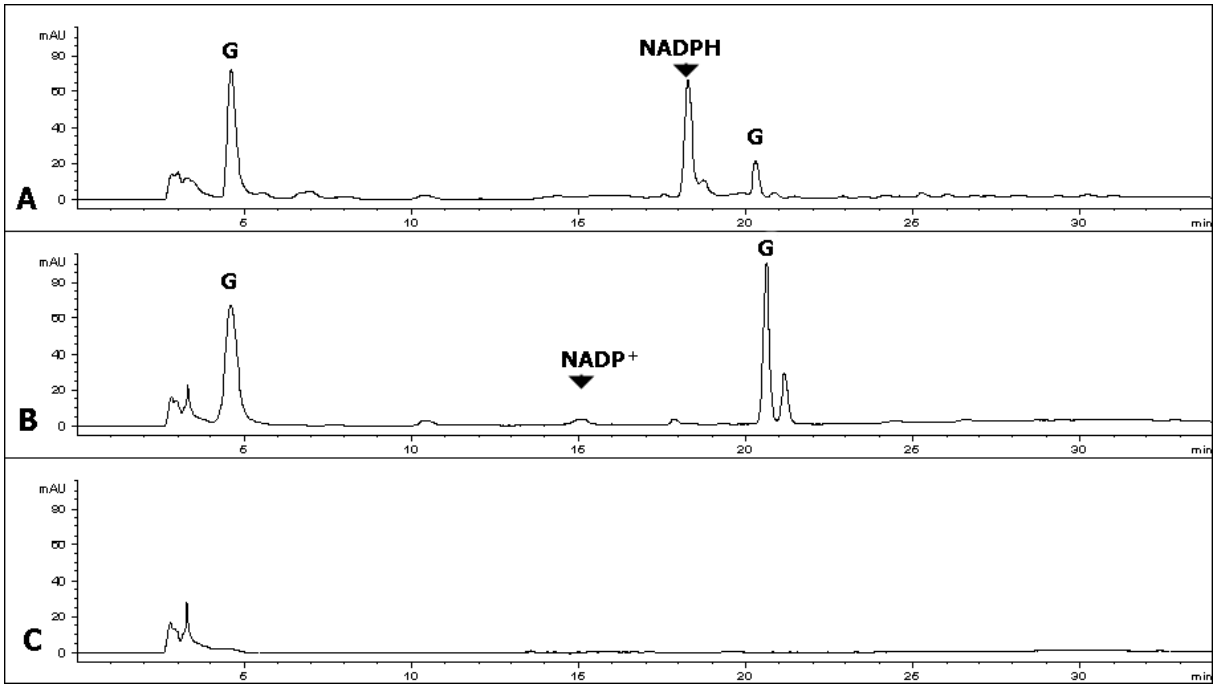

Figure 2 –Supplemental data

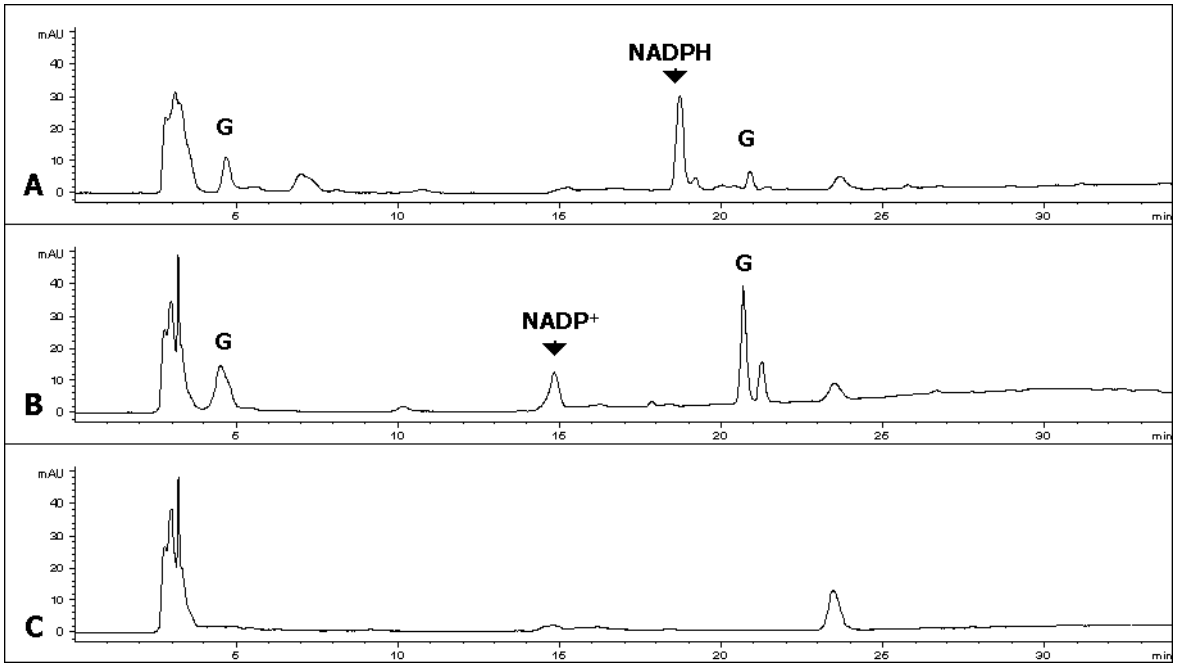

Figure 3 –Supplemental data

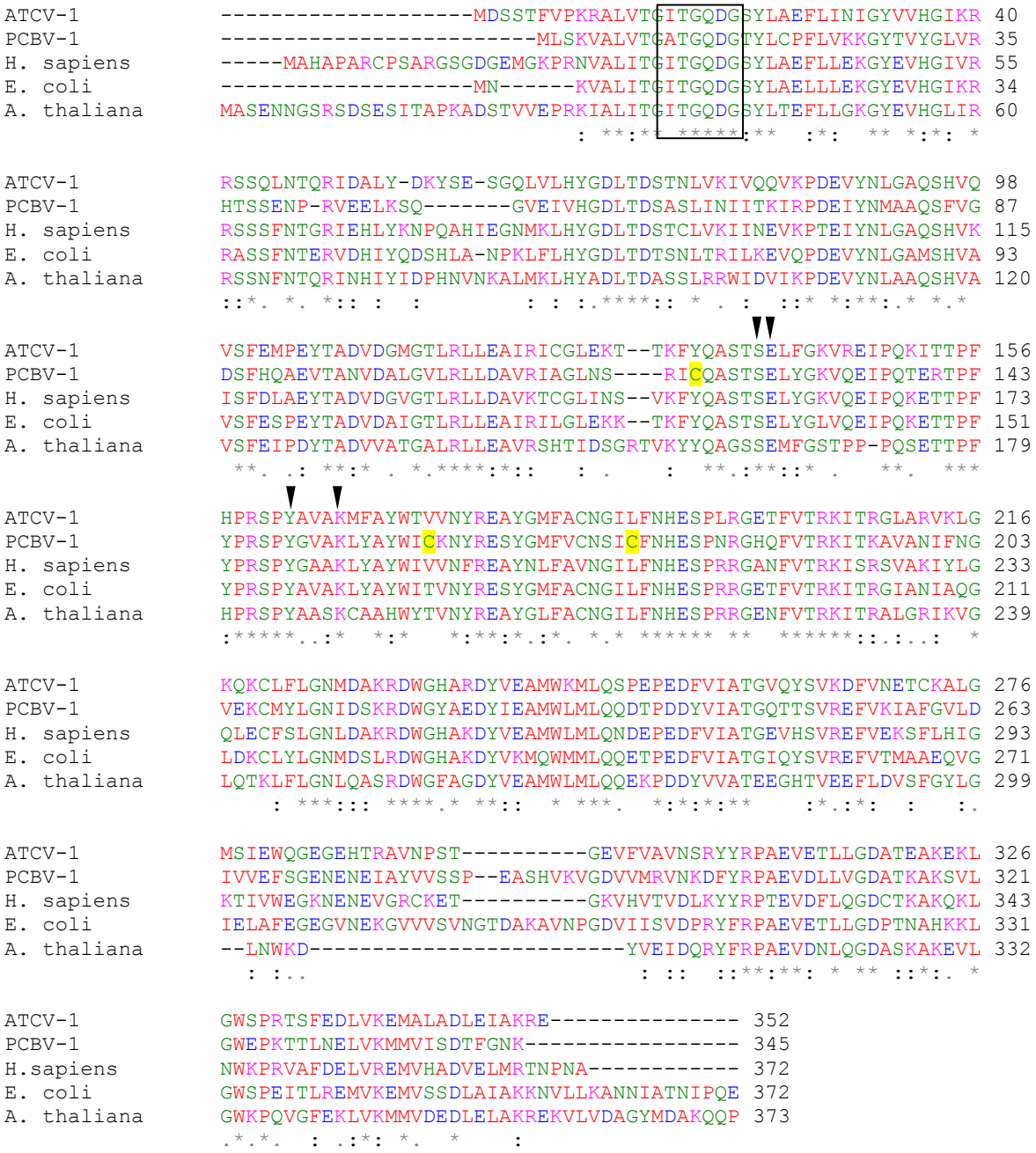

Figure 4 –Supplemental data